

# 2D damping predictions of fiber composite plates: Layup effects

E.K. Billups, M.N. Cavalli \*

*University of North Dakota, Department of Mechanical Engineering, Stop 8359, 243 Centennial Drive, Grand Forks, ND 58202-8359, United States*

Received 29 November 2006; received in revised form 25 May 2007; accepted 12 September 2007

Available online 20 September 2007

## Abstract

Several two-dimensional theories for predicting the specific damping capacity (SDC) of fiber composite laminates are compared. The theories considered are those of Adams and Bacon, Adams and Maheri, Ni and Adams and Saravanos and Chamis. No interlaminar effects are considered. Results show that the theory of Saravanos and Chamis provides the most consistent fit to experimental results for a range of material properties and laminate layups. For some laminates, however, the Saravanos and Chamis method seems to predict the wrong trend in SDC variation versus layup angle. It is not clear from the current work whether this result is due to the absence of interlaminar effects in the theory or the presence of a three-dimensional stress state in the laminate.

© 2007 Elsevier Ltd. All rights reserved.

*Keywords:* A. Polymer–matrix composites; A. Structural materials; B. Modeling; C. Laminate theory

## 1. Introduction

Energy dissipation, or damping, is an important consideration in a variety of engineering designs. Composite materials offer the unique ability to tailor damping behavior, and other properties, for specific applications [1–4]. As a result, composites can be desirable choices in applications as varied as wind turbine blades [5–9], beams and shafts [10,11] and control surfaces [12,13]. A full analysis of damping performance for arbitrary composite structures typically requires three-dimensional numerical analysis due to the mathematical complexity of the problem [14–17]. Simplified, two-dimensional analyses based on the principles of Classical Laminate Theory (CLT) have shown good agreement for particular materials, layups, and geometries, however [1–4,18].

The goal of the current work is to compare several theories available in the literature for predicting the specific damping capacity (SDC) of composite laminates. Theories of Adams and Bacon [1], Ni and Adams [3], Adams and

Maheri [18] and Saravanos and Chamis [19,20] will be examined. Results from each theory will be compared with experimental measurements of SDC values. These comparisons will help illustrate the strengths and shortcomings of each theory as well as the use of two-dimensional damping predictions generally.

An example will then be presented of how the Saravanos and Chamis method can be applied to a composite beam whose plies are assembled at arbitrary angles. Damping, stiffness and deflection predictions for this arbitrary laminate will be presented graphically in several forms, each with specific advantages in terms of selecting a layup for a particular set of design requirements. This example will illustrate the usefulness of the technique in designing fiber composite structures.

## 2. Theory

### 2.1. Overview

All theories compared in this work are based on the assumptions of classical laminate theory for orthotropic materials [21,22]. In short, this implies perfect bonding between plies, no out of plane stresses or strains and small,

\* Corresponding author. Tel.: +1 701 777 4389; fax.: +1 701 777 2271.  
E-mail address: [matthewcavalli@mail.und.nodak.edu](mailto:matthewcavalli@mail.und.nodak.edu) (M.N. Cavalli).

elastic deformations [21,22]. Matrices of applied forces and moments are written as  $[N]$  and  $[M]$ , respectively, with subscripts used to indicate specific components. The typical notation used in this paper for subscripts, unless otherwise noted, is number subscripts, i.e. 1, 2, or 12, are used to denote principal material directions of a lamina while letter subscripts, i.e.  $x$ ,  $y$ , or  $xy$ , denote the global coordinates of the laminate. The two coordinate systems are typically offset by an angle,  $\theta$ .

For elastic deformations, the strain energy stored in each ply can be separated into three components: strain energy in the fiber direction, strain energy transverse to the fiber direction, and strain energy in shear. Some amount of each of these components is dissipated during deformation. One way to quantify this dissipation is by using the specific damping capacity which is defined as the strain energy dissipated during a stress cycle,  $\Delta U$ , divided by the maximum strain energy during a stress cycle, Eq. (1).

$$\psi = \frac{\Delta U}{U_{\max}} \quad (1)$$

The total strain energy dissipated for each lamina is the product of the lamina strain energy components with the damping coefficient for the appropriate mode of deformation, all integrated over the thickness of the ply. Consequently, this method requires knowledge of three damping coefficients for each lamina: the longitudinal (fiber direction) coefficient,  $\psi_{L_k}$ , the transverse coefficient,  $\psi_{T_k}$ , and the in-plane shear coefficient,  $\psi_{LT_k}$ , where the subscript  $k$  denotes these are the properties of the  $k$ th lamina. The damping coefficients can be determined via tests on unidirectional laminates under various angles of loading. The energy dissipation can be summed over the total number of plies and, using the total energy dissipated in the laminate, the overall specific damping capacity (SDC) written as [1]:

$$\psi_{\text{laminate}} = \psi_1 + \psi_2 + \psi_{12} \quad (2)$$

## 2.2. Adams and Bacon theory

Adams and Bacon [1] presented a general equation to predict the SDC of beams for applied forces,  $\{N\}$ , and moments,  $\{M\}$ . The equation can be used for any laminate configuration and the lamina damping coefficients ( $\psi_{L_k}$ ,  $\psi_{T_k}$ ,  $\psi_{LT_k}$ ) are allowed to be stress dependent:

$$\psi_{\text{laminate}} = \frac{2 \sum_{k=1}^n \int_{h_{k-1}}^{h_k} (\delta(\Delta U_1) + \delta(\Delta U_2) + \delta(\Delta U_{12})) dz}{\{N\}^T \{\varepsilon^o\} + \{M\}^T \{\kappa\}} \quad (3)$$

Eq. (3) includes contributions from all in-plane stresses but does not allow for out-of-plane contributions to energy dissipation. The latter limitation is consistent for all theories presented in this paper. The number of terms involved in Eq. (3) leads to a level of complexity that can typically only

be handled using numerical techniques. Adams and Bacon recognized this and derived several approximations to Eq. (3) that lend themselves to easier solutions by neglecting certain stresses and strains or limiting the allowable layups [1].

## 2.3. Ni and Adams theory

Additional damping prediction equations were developed by Ni and Adams [3]. They assumed free flexure deformation, stress-independent damping coefficients and a symmetric layup [3]. This final assumption leads to no midplane strains under classical laminate plate theory. In addition to neglecting  $\sigma_y$  and  $\tau_{xy}$ , Ni and Adams also argued that the transverse strain,  $\varepsilon_y$ , in each lamina will be much smaller than the longitudinal and shear strains and could be neglected [3], resulting in Eqs. (4)–(6)

$$\psi_1 = \frac{8\psi_L}{C_{11}p^3} \sum_{k=1}^{p/2} m^2 (\mathcal{Q}_{11}^k C_{11} + \mathcal{Q}_{12}^k C_{12} + \mathcal{Q}_{16}^k C_{16}) \times (m^2 C_{11} + mn C_{16}) W_k \quad (4)$$

$$\psi_2 = \frac{8\psi_T}{C_{11}p^3} \sum_{k=1}^{p/2} n^2 (\mathcal{Q}_{11}^k C_{11} + \mathcal{Q}_{12}^k C_{12} + \mathcal{Q}_{16}^k C_{16}) \times (n^2 C_{11} - mn C_{16}) W_k \quad (5)$$

$$\psi_{12} = \frac{8\psi_{LT}}{C_{11}p^3} \sum_{k=1}^{p/2} mn (\mathcal{Q}_{11}^k C_{11} + \mathcal{Q}_{12}^k C_{12} + \mathcal{Q}_{16}^k C_{16}) \times (2mn C_{11} - (m^2 - n^2) C_{16}) W_k \quad (6)$$

where  $[C]$  is the normalized flexural compliance of the laminate,  $[\mathcal{Q}^k]$  is the stiffness of the  $k$ th lamina,  $p$  is the total number of plies present in the laminate and  $W_k$  is a weighting factor based on the position of the  $k$ th lamina within the laminate [3].

## 2.4. Adams and Maheri theory

Revisions to the Ni and Adams equations were made by Adams and Maheri [18]. The derivation of the equation deviated from the method used by Ni and Adams but the final result is similar. In short, the Adams and Maheri theory is the Ni and Adams theory with slight notational changes and the transverse lamina strain,  $\varepsilon_y$ , term included [18].

## 2.5. Saravanos and Chamis theory

The expression for the strain energy of a general laminate under general loading has been formulated by Tse and Lai [23] and Saravanos and Chamis [19]. Saravanos and Chamis have also written the three SDC components in matrix form [19,20]. These results can be combined to give an expression for the SDC of an arbitrary laminate under general loading which can be written as

$$\psi_{\text{laminate}} = \frac{\begin{Bmatrix} N \\ M \end{Bmatrix}^T \left( \begin{bmatrix} A^* & B^* \\ C^* & D^* \end{bmatrix} \right)^T \begin{bmatrix} A_D & B_D \\ B_D & D_D \end{bmatrix} \left( \begin{bmatrix} A^* & B^* \\ C^* & D^* \end{bmatrix} \right) \begin{Bmatrix} N \\ M \end{Bmatrix}}{\begin{Bmatrix} N \\ M \end{Bmatrix}^T \left( \begin{bmatrix} A^* & B^* \\ C^* & D^* \end{bmatrix} \right)^T \begin{Bmatrix} N \\ M \end{Bmatrix}} \quad (7)$$

where  $A^*$ ,  $B^*$ ,  $C^*$  and  $D^*$  represent the components of the inverse of the original material stiffness matrix [21,22].  $A_D$ ,  $B_D$ ,  $C_D$  and  $D_D$  are the components of the original stiffness matrix multiplied by appropriate damping coefficients.

Eq. (7) is the basis of the Saravanos and Chamis theory. It should be noted that in their original work, Saravanos and Chamis also include the possibility of interlaminar effects, but those are not considered here [21,22]. Though it is not perhaps immediately apparent, the form of the Saravanos and Chamis theory expression for laminate damping is very similar in form to that previously developed by Adams and Bacon (Eq. (3)). An important distinction is that Eq. (7) is written in terms of stiffnesses and strains while Eq. (3) is written in terms of stresses and compliances. This made sense for Adams and Bacon because they included stress-dependence in their damping coefficients which the Saravanos and Chamis theory does not. The tradeoff, however, is that the Adams and Bacon form is less computationally efficient.

### 3. Results and discussion

#### 3.1. Comparison with previous work

Experimentally determined values for the specific damping coefficients were obtained from the literature for several variations of E-glass–epoxy and carbon–epoxy fiber composites under free-free flexural loading [1–3]. Table 1 lists the material properties for each laminate [1–3]. These values were used in the Ni and Adams [3], Adams and Maheri [2] and Saravanos and Chamis [19] theories to calculate the predicted values of SDC for various fiber geometries.

All calculations were performed using MATLAB (The Mathworks, Natick, MA). Unfortunately, the general theory of Adams and Bacon can only be compared with the

data presented in the original paper [1]. This is because the theory allows for stress dependent damping coefficients but does not explicitly identify the relationship between the coefficients and the lamina stresses. The results of Adams and Bacon could thus not be recalculated for other laminate geometries. Transcription of data points from the original plots has been used to recreate their curves in the current work.

Adams and Maheri [2] measured the specific damping capacity of two laminate configurations of Fibredux 913/glass fiber composites. The first was a balanced symmetric angle-ply laminate,  $[-\theta^\circ/+\theta^\circ/-\theta^\circ/+\theta^\circ]_s$  and the second was a symmetric unidirectional laminate,  $[\theta^\circ]_8$ . Beams were cut from plates with the above layups and excited at the fundamental flexural mode of vibration. The variation of the SDC with fiber orientation for these configurations is shown in Figs. 1 and 2, respectively. Note that results from two beam widths are plotted in Fig. 1. No experimental uncertainty is presented with the original data, but the beam width does not appear to cause a dramatic effect on the damping [2]. Results from Kyriazoglou and Guild indicate this may not be the case for larger ranges of aspect ratios [24]. All theories predict the SDC values reasonably well for both laminates. The blank legend symbol for the Adams/Maheri theory indicates that this theory is identical to the theory listed above it (Saravanos, in this case) for this particular laminate.

Figs. 3 and 4 show results from experiments conducted by Adams and Bacon [1] on DX209/carbon fiber composite laminates. The layup in Fig. 3 is  $[\theta]_{10}$  and the layup in Fig. 4 is  $[\theta]_5$ . No information is given regarding the difference between experimental data sets 1 and 2 in Fig. 3 [1]. The Saravanos and Chamis theory and the Adams and Bacon theory provide the most consistent fit in terms of both magnitude of the predicted SDC and shapes of the curves. Fig. 4 shows that there are some layup/material

Table 1  
Material properties for damping results presented.

Material		$E_1$ (ksi GPa)	$E_2$ (ksi GPa)	$G_{12}$ (ksi GPa)	$\nu_{12}$	$\psi_L$ (%)	$\psi_T$ (%)	$\psi_{LT}$ (%)	$V_f$	References
Fiber	Matrix									
E-glass	Epoxy (DX 210)	5480	1580	712	0.29	0.87	5.05	6.91	0.5	[3]
		37.8	10.9	4.91						
E-glass	Epoxy (Fibredux 913)	6020	1810	730	0.2	1.61	6.7	7.3	0.54	[2]
		41.5	12.5	5.03						
HMS carbon	Epoxy (DX 209)	27,400	882	395	0.3	0.64	6.9	10		[1]
		189	6.08	2.72						
HMS carbon	Epoxy (DX 210)	25,000	1040	545	0.29	0.45	4.22	7.05	0.5	[3]
		172	7.17	3.76						

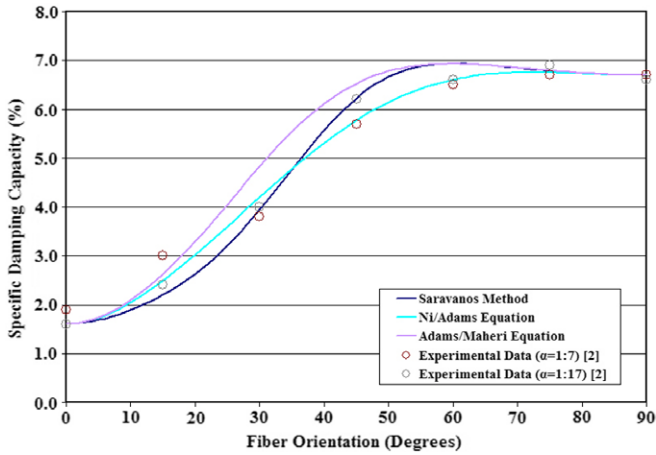


Fig. 1. Variation of the specific damping capacity with fiber orientation for a glass/epoxy (Fiberdux 913G) laminate with a “symmetric” angle-ply layup of  $[-\theta^\circ/+\theta^\circ/-\theta^\circ/+\theta^\circ]$ .

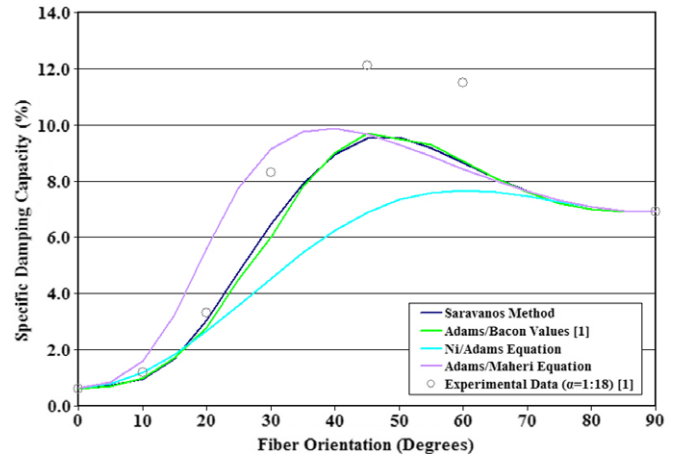


Fig. 4. Variation of the specific damping capacity with fiber orientation for carbon/epoxy (HMS/DX209) laminate with a angle ply layup of  $[\theta^\circ/-\theta^\circ]_5$ .

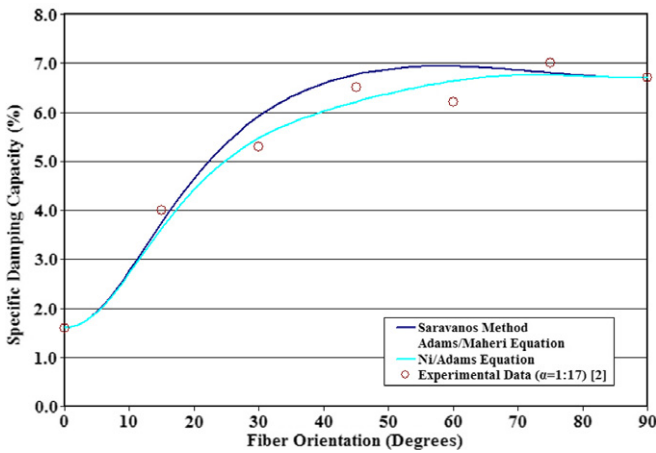


Fig. 2. Variation of the specific damping capacity with fiber orientation for a glass/epoxy (Fiberdux 913G) laminate with a unidirectional layup of  $[\theta^\circ]_8$ .

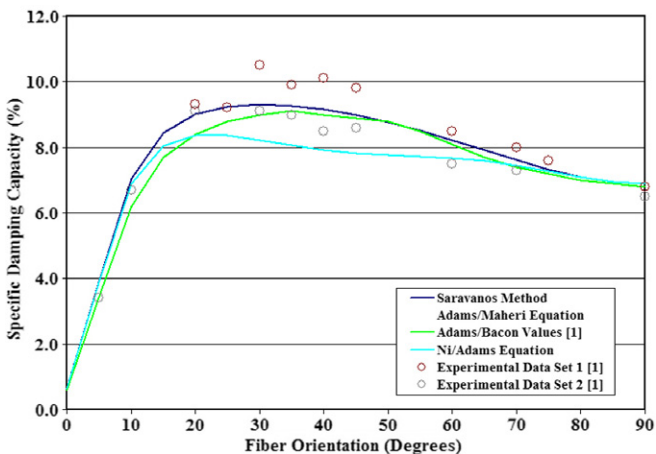


Fig. 3. Variation of the specific damping capacity with fiber orientation for carbon/epoxy (HMS/DX209) laminate with a unidirectional layup of  $[\theta^\circ]_{10}$ .

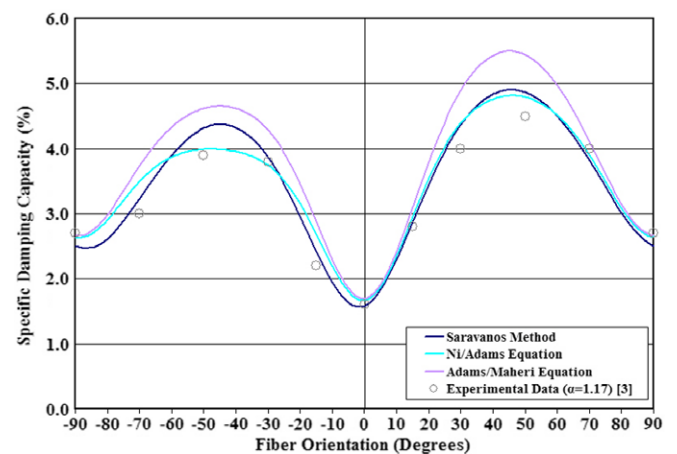


Fig. 5. Variation of the specific damping capacity with outer ply fiber orientation for a glass/epoxy (glass/DX210) laminate with a layup of  $[\theta^\circ/(\theta+90)^\circ/(\theta+45)^\circ/(\theta-45)^\circ]$ .

combinations where the 2D theories are not able to fully predict the behavior of the material. This may be due to interlaminar effects or may indicate that a three-dimensional stress state exists for this laminate. Since no uncertainty is quoted on the experimental data, however, no firm conclusion can be reached.

Ni and Adams [3] investigated symmetric laminates,  $[\theta^\circ/(\theta+90)^\circ/(\theta+45)^\circ/(\theta-45)^\circ]_s$ , for both glass and carbon fibers with DX210 epoxy. The width-to-length ratios of the beams used in the experimental damping determination was 1:17. The variation of the SDC with respect to the outer ply orientation for a glass and carbon composites is shown in Figs. 5 and 6, respectively. The damping trend is captured reasonably well by all theories for the glass fiber composite but significant discrepancies are apparent for the carbon fiber material. Both the Adams and Maheri and Ni and Adams theories significantly overpredict the damping for positive angles and neither capture the shape of the SDC curve for positive

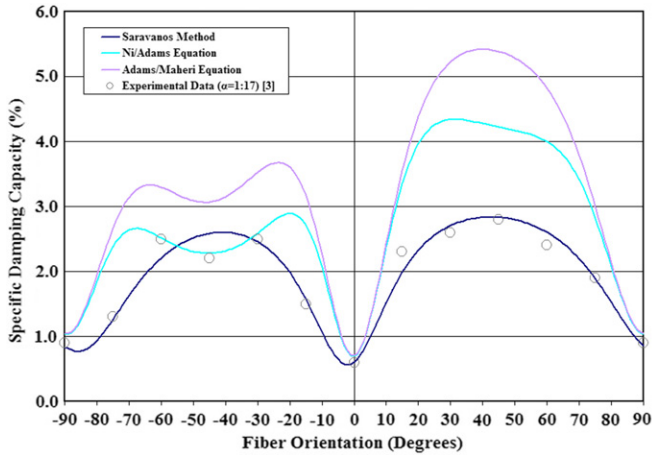


Fig. 6. Variation of the specific damping capacity with outer ply fiber orientation for a carbon/epoxy (HMS/DX210) laminate with a layup of  $[\theta^\circ/(\theta + 90)^\circ/(\theta + 45)^\circ/(\theta - 45)^\circ]$ .

values of  $\theta$  as well as the Saravanos and Chamis theory. For negative values of  $\theta$ , both Adams and Maheri and Ni and Adams again overpredict the measured damping. The Saravanos and Chamis theory gives reasonable predictions for the SDC magnitude at negative values of  $\theta$ , but seems to predict the wrong shape for the SDC curve near  $\theta = -45^\circ$ . It is not clear if the discrepancies between the theory and data for this laminate arise from uncertainty in the experimental results, edge effects, interlaminar effects or a three-dimensional stress state.

Fig. 7 shows an interesting result for the Adams and Maheri theory applied to the  $[\theta^\circ/(\theta + 90)^\circ/(\theta + 45)^\circ/(\theta - 45)^\circ]$  carbon/DX210 laminate. The  $\psi_2$  component of the SDC is plotted versus outer ply orientation. For some orientations, the Adams and Maheri theory actually predicts negative values of  $\psi_2$ , an unrealistic result that implies energy generation, rather than damping. Values

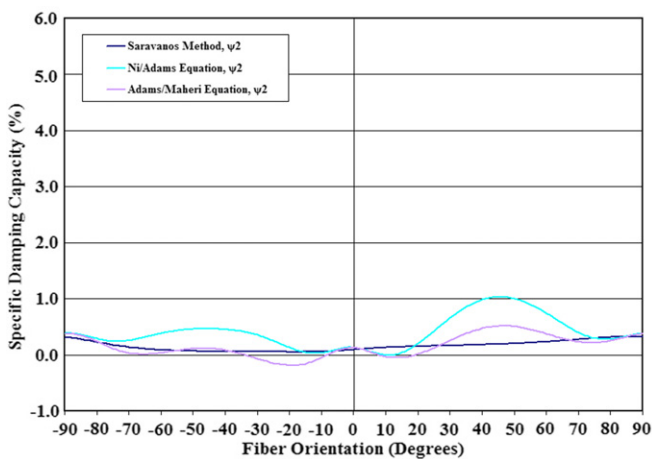


Fig. 7. Variation of the specific damping capacity component  $\psi_2$  with outer ply fiber orientation for a carbon/epoxy (HMS/DX210) laminate with a layup of  $[\theta^\circ/(\theta + 90)^\circ/(\theta + 45)^\circ/(\theta - 45)^\circ]$ .

of  $\psi_2$  are positive for all orientations in the Ni and Adams and Saravanos and Chamis theories but the shapes of the two curves are significantly different. These differences can be traced back to the fundamentally different assumptions regarding stresses and strains within the plies.

### 3.2. Predictions of damping for arbitrary laminates

The Saravanos and Chamis theory will now be applied to an arbitrary laminate to illustrate the information that can be provided regarding composite laminate properties. Values from Table 1 for the Ni and Adams Fibredux 913/glass fiber damping coefficients will be used for all predictions [3]. The laminate to be analyzed is of the form  $[\theta_1^\circ/(\theta_1 + \alpha)^\circ/(\theta_1 - \alpha)^\circ/(\theta_1 + \alpha)^\circ/(\theta_1 - \alpha)^\circ/(\theta_2 - \alpha)^\circ/(\theta_2 + \alpha)^\circ/(\theta_2 - \alpha)^\circ/(\theta_2 + \alpha)^\circ/\theta_2^\circ]$ , where  $\theta_1$ ,  $\theta_2$ , and  $\alpha$  could take on any value from  $0^\circ$  to  $180^\circ$ .

First, let us select a single value for the offset angle,  $\alpha = 90^\circ$ . Fig. 8 illustrates how the SDC of the resulting laminate varies with changes in  $\theta_1$  and  $\theta_2$  under  $M_x$  loading. The maximum possible value of SDC is approximately 5.7% and occurs when  $\theta_1 = 48^\circ$  and  $\theta_1 = 132^\circ$ . Note that the resolution of Fig. 8 for both  $\theta_1$  and  $\theta_2$  is  $2^\circ$ . The minimum level of damping that can be achieved in this laminate is about 1.7%, when  $\theta_1 = \theta_2 = 90^\circ$ . Referring to Table 1, most energy in this material is dissipated by deformations in the matrix, so both of these results make sense. Values of  $\theta_1$  and  $\theta_2$  near  $45^\circ$  result in a large contribution from matrix deformation and lead to large overall values of energy dissipation. In contrast, values of  $\theta_1$  and  $\theta_2$  near  $90^\circ$  result in most of the laminate (8 of 10 plies) having

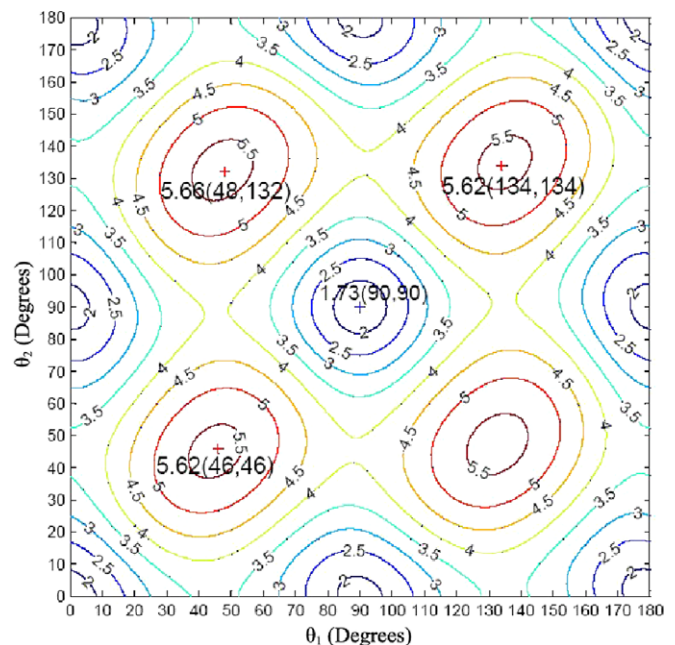


Fig. 8. Variation of SDC (%) prediction with fiber orientation angle for glass/epoxy in a symmetric layup of  $[\theta_1^\circ/(\theta_1 + 90)^\circ/(\theta_1 - 90)^\circ/(\theta_1 + 90)^\circ/(\theta_1 - 90)^\circ/(\theta_2 - 90)^\circ/(\theta_2 + 90)^\circ/(\theta_2 - 90)^\circ/(\theta_2 + 90)^\circ/\theta_2^\circ]$  for  $M_x \neq 0$ .

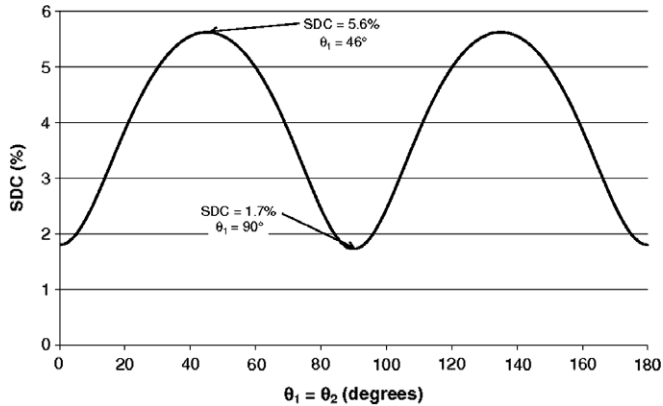


Fig. 9. Variation of SDC (%) prediction with fiber orientation angle for glass/epoxy in a symmetric layup of  $[\theta_1^\circ/(\theta_1 + 90)^\circ/(\theta_1 - 90)^\circ/(\theta_1 + 90)^\circ/(\theta_1 - 90)^\circ]_s$ , for  $M_x \neq 0$ .

the fiber direction aligned along the  $x$ -axis. This leads to very little damping contribution from matrix deformations and minimizes the overall energy dissipation.

It is necessary to recognize that the value of the SDC may not be the only laminate property of interest. If a laminate deforms in an undesirable way during loading or curing (e.g. warps), it may not be able to fulfill its design requirements despite desirable energy dissipation characteristics. Similarly, the laminate must possess the proper effective stiffness under a given mode of loading. Contours showing laminate effective stiffness and warpage behavior as a function of layup geometry can be created easily by incorporating the appropriate equations into the MATLAB code. These can then be compared with the SDC-layup contour (Fig. 8) to optimize the composite layup.

It is possible that the entire design space of Fig. 8 is not attainable or desirable in a given manufacturing situation. The simplicity of a symmetric layup may be desirable, for example. In such a situation, a second method of analyzing the Saravanos and Chamis theory results would be to pull out SDC values along a specified section of Fig. 8. For a symmetric laminate, Fig. 9 is the result. Fig. 9 indicates that values of  $\theta_1$  must be between  $31^\circ$  and  $59^\circ$  to achieve damping within about 10% of the maximum value for a symmetric laminate. To be within about 10% of the minimum value,  $\theta_1$  must be between  $85^\circ$  and  $95^\circ$ . Corresponding sections could be constructed for various conditions ( $\theta_1 = \text{constant}$ ,  $\theta_2 = \text{constant}$ ,  $\theta_1/\theta_2 = \text{constant}$ , etc.).

A third method of using the Saravanos and Chamis technique is to allow all angles,  $\theta_1$ ,  $\theta_2$ , and  $\alpha$ , to vary from  $0^\circ$  to  $180^\circ$ . This method allows the full range of laminate properties that can be achieved to be identified. Fig. 10 shows the range of SDC that are predicted for this laminate as a function of the effective flexural stiffness. The maximum achievable value of SDC is approximately 6% and occurs in a laminate with  $\theta_1 = \theta_2 = 48^\circ$  and  $\alpha = 0^\circ$ . Minimum damping ( $\sim 0.8\%$ ) occurs in a laminate with  $\theta_1 = \theta_2 = \alpha = 0^\circ$ . The fact that the maximum damping is

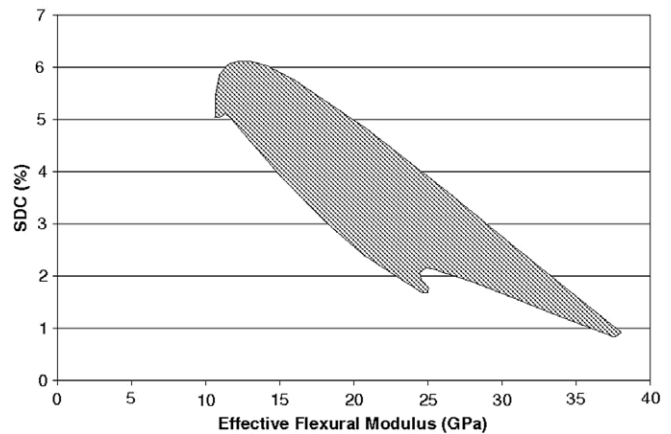


Fig. 10. SDC – flexural modulus envelope showing all possible combinations predicted by CLT theory for glass/epoxy laminate with layup  $[\theta_1^\circ/(\theta_1 + \theta)^\circ/(\theta_1 - \theta)^\circ/(\theta_1 + \theta)^\circ/(\theta_1 - \theta)^\circ/(\theta_2 - \theta)^\circ/(\theta_2 + \theta)^\circ/(\theta_2 - \theta)^\circ/(\theta_2 + \theta)^\circ/\theta_2^\circ]$ .

in a layup of approximately  $\pm 45^\circ$  and the minimum damping is in the stiffest laminates is not surprising given the material properties. What makes Fig. 10 interesting is the fact that it clearly shows that for a given value of effective stiffness, it may be possible to tailor the SDC of the laminate over a relatively large range. Similar design envelopes can be defined for other types of loadings as well as laminate out-of-plane deformations. The calculations required to construct Fig. 10 resulted in approximately 26,000 data points and required approximately 45 minutes to complete on a 3GHz Pentium 4 PC. With the information from the CLT method presented in this form, damping, stiffness and warpage of potential laminates can be quickly assessed.

#### 4. Conclusions

A comparison of the damping predictions from several two-dimensional composite laminate theories has been conducted. Results indicate that the general theory of Saravanos and Chamis most consistently agrees with experimental results. Certain layup/material combinations show significant deviations between theoretical predictions and experimental data, particularly with stiffer carbon reinforcement. More work is needed to determine whether these differences arise from interlaminar, edge or three-dimensional stress effects.

The Saravanos and Chamis method has been used to predict the damping, stiffness and out-of-plane deformation for an arbitrary composite laminate. Several approaches to the analysis are presented to quickly identify the performance envelope of a specific laminate and to tailor properties such as the specific damping coefficient (SDC) and the effective stiffness. These approaches could be applied to structures such as wind turbine blades where energy dissipation and stiffness both play a large role in successful design performance.

## Acknowledgement

Financial support of Mr. Billups from the UND Mechanical Engineering Department during the course of this work is gratefully acknowledged.

## References

- [1] Adams RD, Bacon DGC. Effect of fibre orientation and laminate geometry on the dynamic properties of CFRP. *J Compos Mater* 1973;7:402–28.
- [2] Adams RD, Maheri MR. Dynamic flexural properties of anisotropic fibrous composite beams. *Compos Sci Technol* 1994;50(4):497–514.
- [3] Ni RG, Adams RD. The damping and dynamic moduli of symmetric laminated composite beams – theoretical and experimental results. *J Compos Mater* 1984;18(2):104–21.
- [4] Chandra R, Singh SP, Gupta K. Damping studies in fiber-reinforced composites – a review. *Compos Struct* 1999;46:41–51.
- [5] Bechly ME, Clausen PD. Structural design of a composite wind turbine blade using finite element analysis. *Comput Struct* 1999;63(3):639–46.
- [6] Lobitz D, Veers PS, Migliore PG. Enhanced performance of HAWTs using adaptive blades. In: *Proceedings of the wind 1996 ASME wind energy symposium*. Houston, Texas, USA: ASME; 1996.
- [7] Lee AT, Flay RGJ. Compliant blades for wind turbines. *The Inst Prof Eng New Zealand* 1999;26(1):7–12.
- [8] Garfinkle M. Twisting smartly in the wind. *Aerospace Amer* 1994;32(7):18–20.
- [9] Chandra R. Active shape control of composite blades using shape memory actuation. *Smart Mater Struct* 2000;10(5):1018–34.
- [10] Bert CW, Kim C. Whirling of composite-material driveshafts including bending-twisting coupling and transverse shear deformation. *J Vibr Acoust* 1995;117(1):17–21.
- [11] Lentz WK, Armaios EA. Optimum coupling in thin-walled, closed-section composite beams. *J Aerospace Eng* 1998;11(3):81–8.
- [12] Klous H, Mirza S. Piezoelectric induced bending and twisting of laminated composite shallow shells. *Smart Mater Struct* 2000;9(4):476–84.
- [13] Kim C, Park B-S, Goo N-S. Shape changes by coupling bending and twisting of shape-memory-alloy-embedded composite beams. *Smart Mater Struct* 2002;11(4):519–26.
- [14] Wetherhold RC, Panthalingal N. Piezoelectric PZT/epoxy composites for controlling torsional motion. *J Intell Mater Syst Struct* 1994;5:576–80.
- [15] Chandra R, Singh SP, Gupta K. A study of damping in fiber-reinforced composites. *J Sound Vibr* 2003;262:475–96.
- [16] Hwang SJ, Gibson RF. The effects of three-dimensional states of stress on damping in laminated composites. *Compos Sci Technol* 1991;41:379–93.
- [17] Hwang SJ, Gibson RF. Influence of bending-twisting and extension-bending coupling on damping of laminated composites. *J Mater Sci* 1993;28:1–8.
- [18] Adams RD, Maheri MR. Damping in advanced polymer–matrix composites. *J Alloys Comp* 2003;355(1–2):126–30.
- [19] Saravanos DA, Chamis CC. Unified micromechanics of damping for unidirectional fiber reinforced composites, NASA TM-102107. National Aeronautics and Space Administration, Cleveland; 1989.
- [20] Saravanos DA, Chamis CC. Mechanics of damping for fiber composite laminates including hygro-thermal effects, NASA TM-102329. National Aeronautics and Space Administration, Cleveland; 1989.
- [21] Jones RM. *Mechanics of composite materials*. Philadelphia: Taylor & Francis; 1999.
- [22] Kaw AK. *Mechanics of composite materials*. Boca Raton, Florida: CRC Press; 1997.
- [23] Tse PC, Lai TC. Expression for the strain energy of laminated composite thin shells. *Int J Mech Eng Educ* 1995;23(2):169–77.
- [24] Kyriazoglou C, Guild FJ. Finite element prediction of damping of composite GFRP and CFRP laminates – a hybrid formulation – vibration damping experiments and Rayleigh damping. *Compos Sci Technol* 2006;66(3–4):487–98.